Proposal for measuring line profiles and angular distributions of the radiative-electron-capture transition in low-energy ion-atom collisions: Beyond the impulse approximation

Tian Li and Deyang Yu*

Institute of Modern Physics, Chinese Academy of Sciences, Lanzhou 730000, China
and University of Chinese Academy of Sciences, Beijing 100049, China

(Received 4 November 2021; accepted 1 March 2022; published 16 March 2022)

We propose to measure line profiles and angular distributions of the radiative-electron-capture transition in collisions of sub-MeV/u Ar^{18+} with helium. We estimate the line profile and the angular distribution using hydrogenlike and Hartree-Fock wave functions and show that the asymmetry of the line profile and the deviation of the angular distribution from the $\sin^2\theta_t$ law are magnified in the sub-MeV/u region. Finite detector resolution and ion-beam monochromaticity are considered, and the results show that by using a usual bent-crystal spectrometer and a group of commercial silicon drift x-ray detectors one will be able to obtain sufficiently precise line profile and angular distribution to distinguish different theoretical descriptions of target atoms. The enhanced sensitivity to different theoretical approaches at low energies suggests that the proposed experiment will provide insights into the electromagnetic transition of an electron between a pair of relatively moving nuclei.

DOI: 10.1103/PhysRevA.105.032810

I. INTRODUCTION

Radiative electron capture (REC) [1–3] is one of the fundamental processes in ion-atom collisions, in which a bound electron in a target atom is transferred to a projectile ion and simultaneously a photon is emitted to carry excess energy and to fulfill the law of momentum conservation. Raisbeck and Yiou exhibited a hint of REC by measuring the capture cross sections of high-energy protons [4]. Soon after that, K-REC (i.e., the target electron is transferred directly to a K-shell vacancy of the projectile ion) photons were observed in the penetration of fast heavy ions through various foils by Schnopper *et al.* [5] and also in collisions of fast highly charged ions (HCIs) with noble gases by Kienle *et al.* [6]. Thereafter, REC has been extensively studied both experimentally [7–17] and theoretically [18–38]. It has been shown that the K-REC process dominates the L- and M-REC processes [3].

Nevertheless, in all performed REC experiments, the projectiles were always acted by high-energy ions. On the one hand, the use of low-energy light ions causes a poor signal-to-noise ratio since the REC photon energy is low and usually overlaps with backgrounds. On the other hand, it is very difficult to obtain an intense low-energy bare or hydrogenlike heavy-ion beam as the stripper-foil technique works efficiently only for high-energy heavy ions, and the electron beam ion sources provide very weak beams of this kind. In those high-energy experiments, the projectile velocity is much higher than the orbital velocity of the target electrons and, thus, the REC process can be well described within the impulse approximation [1–3,19]. This description is based on the radiative recombination (RR) process, in which the capture process is treated as a transition of a quasifree electron from a continuum state to a bound (e.g., the ground) state in the projectile frame. The momentum of target electrons contributes to the REC photon energy via its kinetic energy relative to the projectile and, therefore, the energy-differential REC cross sections $d\sigma^{REC}/d\omega$ are essentially convolutions between the RR cross sections $\sigma^{RR}(\varepsilon_e)$ and the distributions $\rho(\varepsilon_r)$ of the relative kinetic energies of the target electrons. Here, ε_e represents the kinetic energy of the incident electron involved in the RR process, and ε_r is the kinetic energy of the target electron with respect to the projectile ion. An obvious inference is that the REC line profile characterizes the target electron wave function, as discussed by Ichihara *et al.* [26]. In the high-energy region, the relative kinetic energy of the electron originates mainly from the relative velocity of the projectile ion and the target nucleus rather than the relative velocity of the electron and the target nucleus, and the RR cross sections decrease monotonically and slowly with the kinetic energy of the electron. These make the energy distribution of REC photons exhibit a wide, symmetric, and Lorentz-like profile [12,13,26,39,40]. Moreover, for the collisions of low- and medium-Z projectile ions with nonrelativistic velocities, the dipole approximation of the electromagnetic transition is valid, and therefore the angular distribution of the REC photons obeys the $\sin^2\theta_t$ law [10], where θ_t is the angle between the directions of the REC photon and the projectile ion in the target frame.

Due to recent progress on a low-energy HCI accelerator with a new-generation superconducting electron cyclotron resonance ion source (ECRIS), ion beams of 0.3–0.7 MeV/u Ar^{18+} with intensity up to microamperes are expected to be available in the near future [41]. Therefore, experimental studies on the corresponding REC process with a photon energy range 4.3–5.1 keV will become possible using a usual bent-crystal spectrometer [42–44] for its line profile and a group of

*Corresponding author: d.yu@impcas.ac.cn

commercial silicon drift x-ray detectors [45] for its angular distribution. In low-energy collisions, since the velocity of target electrons (e.g., about 1.34–2 a.u. for helium) is comparable to the projectile velocity (e.g., 3.5–5.3 a.u., which corresponds to 0.3–0.7 MeV/u), the impulse approximation will lose its appropriateness and significant improvements to theoretical methods are needed in order to accurately describe the REC process under such conditions. The significance of the electron velocity will result in an asymmetry of the line profile and a deviation of the angular distribution from the $\sin^2\theta_t$ law. High-precision experiments will help us to judge and improve future theories.

In low-energy ion-atom collisions, the nonradiative-electron-capture (NRC) process [46] dominates the REC mechanism. Although the NRC process itself does not emit photons, if a transferred electron is populated into an excited state, a photon will be emitted during the subsequent decay. However, because the energy of these photons is lower than that of the K-REC photons, the NRC channels do not contaminate REC measurements.

In the present work we propose an experimental study of the REC process using low-energy projectile ions proceeding from the following considerations.

First, the REC line profile may show an observable asymmetry, although it has not been observed in high-energy collisions yet [12,13,26,39,40]. A similar effect has been observed in low-energy Compton scattering, in which the scattered photons measured at a certain angle demonstrated an asymmetric energy distribution, in spite of being hardly measurable in high-energy photon scattering [47]. In both channels, the momentum distribution of the target electron plays a more important role when the projectile energy becomes lower.

Second, the peak energy of the REC photons may present an extra shift to the low-energy end of the photon-energy spectrum. There are two factors that cause the peak energy of the REC photons to be lower than that of the RR process with the same projectile ions: one is that the target electron involved in REC is initially bounded by the target nucleus and it has a negative energy with respect to a free electron. Another reason is that the transition probability is higher when the relative kinetic energy between the electron and projectile is smaller. This effect will be more significant at low projectile energies because the transition probability increases more severely when the relative kinetic energy decreases.

Third, the polarization effect of the target atom may appear. The wave functions of target atoms can be distorted by the electric field of the highly charged projectile ion, and thus, the relative electron momentum distribution and therefore the REC line profile will be modified. This effect should be more significant in slow collisions due to the longer duration of the ion-atom interaction, and probably can be identified by comparing a precise experimental line profile with a sophisticated theoretical calculation.

Fourth, the REC and the NRC mechanisms may hybridize. In principle, REC is a four-body (i.e., the electron, the two nuclei, and the emitted photon) process. However, in the impulse approximation, the target nucleus and the potential energy of target electrons do not play a dynamic role. The target nucleus acts only to bind the target electron with a certain momentum distribution. In low-energy collisions, since the traveling time of the projectile within the electron orbit becomes longer, the coupling between the nuclei and electron movements plays a more significant role. This can be determined from the domination of NRC in low-energy collisions [1–3]. As an interatomic transition, the REC process occurs during such a strong coupling and, thus, it improves the significance of a hybridization of both the REC and NRC mechanisms, in which the nuclei have a chance to share part of the transition energy. The hybridization will result in a low-energy tail in the REC line profile. A similar process was considered by Voitikov *et al.* in the radiative double-electron-capture process, in which the photon energy is widely distributed because of the coupling between the electron and nuclei movements [48]. However, because of the poor statistics caused by the very small RDEC cross sections, as well as the employment of multishell atoms (e.g., C, N_2, and Ne) as the target resulting in complex x-ray spectra, the effect predicted by Voitikov *et al.* has not been identified by experiments [49,50]. We expect to observe the hybridization between the REC and the NRC mechanisms in slow bare ions with helium collisions since the REC cross section is about a thousand times larger than that of RDEC and the helium atom has only a single shell resulting in a simple x-ray spectrum. Besides, if positronium was used as the target instead of atoms, the hybridization would be expected to be more significant due to the much stronger recoil effect of the positron.

Fifth, the REC line profile and the final target state may entangle. Let us compare the following two K-REC processes:

$$\mathrm{Ar}^{18+} + \mathrm{He} \rightarrow \mathrm{Ar}^{17+}(1s) + \mathrm{He}^{+}(1s) + \gamma_{\mathrm{REC}} \tag{1a}$$

and

$$\mathrm{Ar}^{18+} + \mathrm{He} \rightarrow \mathrm{Ar}^{17+}(1s) + \mathrm{He}^{+*}(2s) + \gamma'_{\mathrm{REC}}. \tag{1b}$$

For these two processes, the corresponding REC line profiles, especially linewidths, should be different due to the significantly different binding energies and thus effective momentum distributions of the transferred electrons. Namely, the REC line profile entangles with the excited state of the recoiled target. A coincidence measurement of both the REC photon and the deexciting photon of the recoiled target will provide a good opportunity to thoroughly investigate dynamical electron-electron correlation in REC processes.

In addition, the angular distribution of REC photons may violate the $\sin^2\theta_t$ law. In nonrelativistic fast ion-atom collisions, the REC photons distribution obeys the $\sin^2\theta_t$ law [2,7]. In relativistic collisions, a violation of this distribution has been employed to probe exotic mechanisms (e.g., the spin-flip process [10–12] and the relativistic effect [26]) when the impulse approximation strictly holds. In low-energy collisions, the transverse velocity of target electrons is comparable to the projectile velocity. In the target frame, it is equivalent to a dispersion of the projectile direction. This will also lead to a violation from the $\sin^2\theta_t$ law but the mechanism is different from that in high-energy collisions.

As discussed above, both the line profile and angular distribution of REC photons carry important information on the

dynamics of interatomic transitions. Even so, the REC process is usually handled in the impulse approximation [1–3], which may lose reliability in the case of low projectile energies. The reformulated impulse approximation (RIA) [51,52] provides a more sophisticated theoretical framework which may extend our understanding of the REC process to the low-energy region. However, a detailed and feasible calculation method for RIA is still lacking, especially when very highly charged projectiles (e.g., the Ar^{18+} ion) and multielectron targets (e.g., the helium atom) are involved. New experiments are indispensable to spawn REC theories in the low-energy regime.

II. ESTIMATIONS OF LINE PROFILE AND ANGULAR DISTRIBUTION

In the impulse approximation, the electron-electron correlation, the polarization of the target atom by the electric field of the projectile ion, and possible dynamical couplings between nuclei movement and electromagnetic transition are disregarded, and thus we cannot judge which factor is the most important under which particular conditions. It should be noted that although the impulse approximation becomes less reliable for low-energy collisions, at present it does offer us information on the sensitivity to different theoretical approaches (e.g., different target wave functions), and help to manage experiments.

In the present work we make estimates using the impulse approximation. Briefly, an expression for the RR differential cross sections reads [3,26]

$$\frac{d\sigma_{\rm ion}^{\rm RR}}{d\Omega} = \frac{1}{2\beta}\frac{\omega^2}{(2\pi)^2}\sum_{s,\lambda,m}|M(\boldsymbol{p},\boldsymbol{k})|^2. \tag{2}$$

Because the mass ratio $m_{\rm ion}/m_{\rm e}$ is treated as infinite, in the ion-rest frame the energy of the RR photon $\omega = \epsilon_i - \epsilon_f$ is independent of its outgoing direction. Here, relativistic units $m_{\rm e} = \hbar = c = 1$ are used. The factor $1/2$ comes from an average over the spin of the incident electron, β is the relative velocity between the ion and the electron, and $M(\boldsymbol{p},\boldsymbol{k})$ denotes the invariant amplitudes:

$$iM(\boldsymbol{p},\boldsymbol{k}) = -ie\int \bar{\psi}_{n\kappa m}\gamma^{\mu}\psi_{\epsilon \boldsymbol{p}s}A_{\mu}^{(k,\lambda)^*}d^3\boldsymbol{r}. \tag{3}$$

Here, $\psi_{\epsilon \boldsymbol{p}s}$, $\psi_{n\kappa m}$, and $A_{\mu}^{(k,\lambda)}$ represent the initial continuous, the final bound wave functions, and the radiation field, respectively. The REC double-differential cross sections are then evaluated by convoluting the RR cross sections with the momentum distributions of the target electron in the projectile frame, which are given by [2,3,19]

$$\frac{d\sigma_{\rm p}^{\rm REC}}{d\omega {\rm d}\Omega} = \int \frac{d\sigma_{\rm ion}^{\rm RR}}{d\Omega}\delta(\epsilon_i - \epsilon_f - \omega)|\phi(\boldsymbol{p},\beta)|^2 d^3\boldsymbol{p}. \tag{4}$$

The REC photon energy is confined by the δ function. Finally, the double-differential cross sections in the target frame can be obtained by the Lorentz transformation [2]:

$$\frac{d^2\sigma_{\rm t}^{\rm REC}}{d\omega {\rm d}\Omega} = \frac{1}{\gamma(1-\beta\cos\theta_{\rm t})}\frac{d\sigma_{\rm p}^{\rm REC}}{d\omega' d\Omega'}, \tag{5}$$

where $\gamma = 1/\sqrt{1-\beta^2}$ is the Lorentz factor.

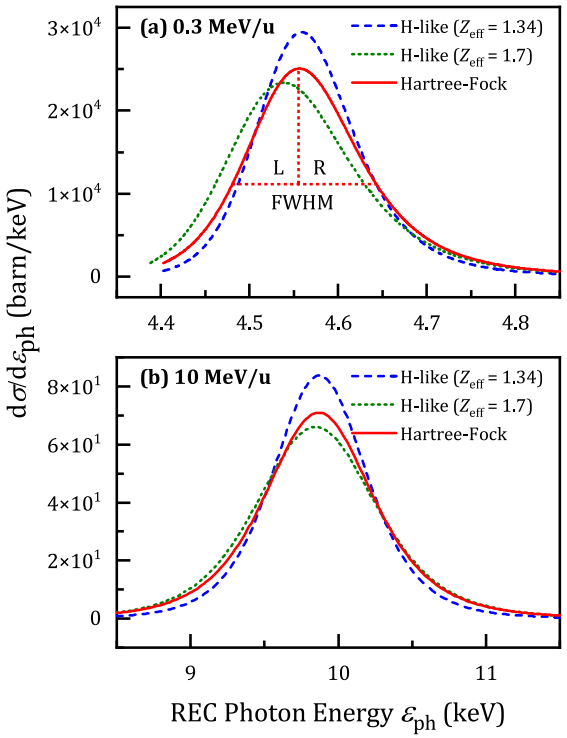

FIG. 1. Line profile of the K-REC transition in collisions of Ar^{18+} with helium at two projectile energies: (a) 0.3 and (b) 10 MeV/u, respectively. The target atom is modeled by hydrogenlike (with $Z_{\rm eff} = 1.34$ and 1.7, which correspond to the first and the average ionization energies of helium) and Hartree-Fock wave functions, respectively. The line profile exhibits significant asymmetry at sub-MeV/u projectile energies.

III. RESULTS AND DISCUSSION

In Fig. 1, we illustrate the line profiles of the K-REC transition in collisions of Ar^{18+} ions with helium for projectile energies of 0.3 and 10 MeV/u. The target atom is described by hydrogenlike (with $Z_{\rm eff} = 1.34$ and 1.7, which correspond to the first and the average ionization energies of helium) and Hartree-Fock wave functions, respectively. Details of the REC line profile indicate an energy changing of the target electron when it transfers in the field of a pair of relatively moving nuclei. A comparison between Figs. 1(a) and 1(b) shows that the profile asymmetry at sub-MeV/u projectile energies is much more significant than that at high energies such as 10 MeV/u, which means that more information is kept at sub-MeV/u projectile energies.

As discussed above, the transverse velocity of target electrons can deform the angular distribution of the REC photons. In Fig. 2(a), one can see that at sub-MeV/u projectile energies the angular distribution deviates from the $\sin^2\theta_{\rm t}$ law, especially at forward (e.g., $\theta_{\rm t} < 30^\circ$) and backward (e.g., $\theta_{\rm t} > 150^\circ$) observation angles. This deviation carries important information on the transverse momentum distribution of target electrons when the transition occurs. In contrast, such an effect is strongly suppressed at high energies such as 10 MeV/u, as shown in Fig. 2(b).

In order to quantify the influences of finite detector resolution and limited beam monochromaticity, we introduce an

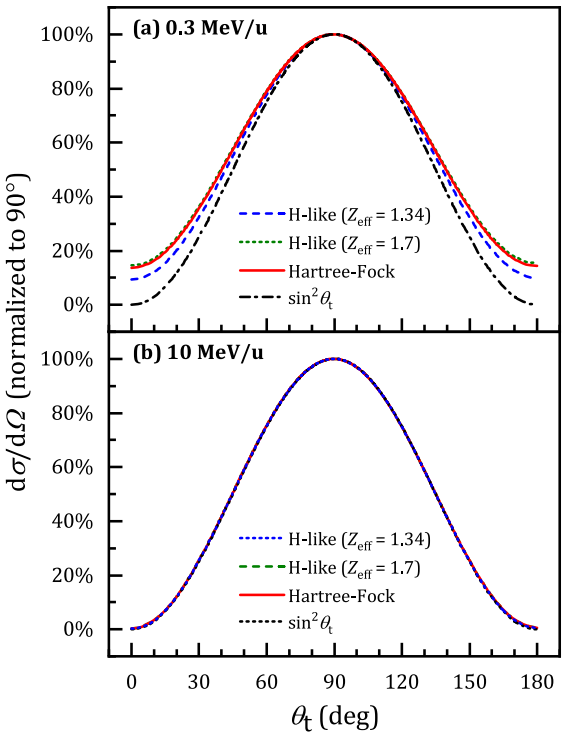

FIG. 2. Angular distribution of the K-REC photons in collisions of Ar^{18+} with helium for two projectile energies: (a) 0.3 and (b) 10 MeV/u, respectively. Descriptions of target atoms are the same as those in Fig. 1. At sub-MeV/u projectile energies the angular distribution deviates from the $\sin^2\theta_t$ law, while at 10 MeV/u this effect disappears.

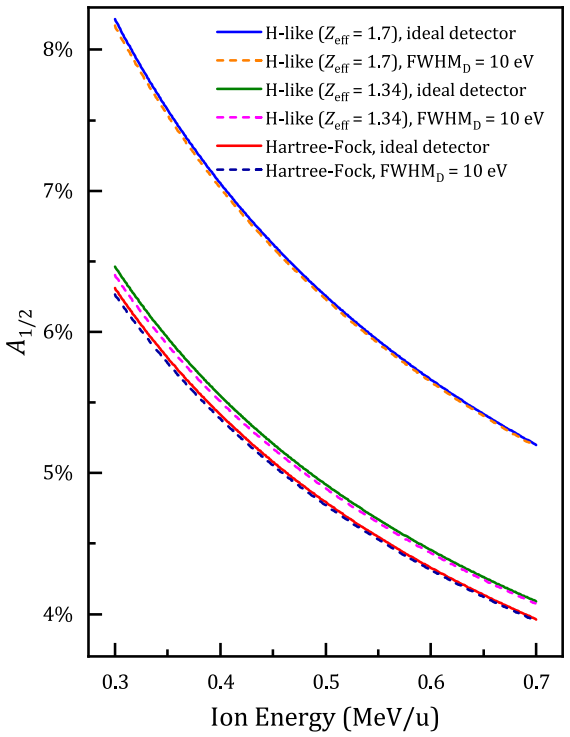

FIG. 3. Influence of detector resolution on asymmetry of the REC line profile in collisions of 0.3–0.7-MeV/u Ar^{18+} with helium. The detector resolution FWHM$_D$ is assumed to be 0 eV for an ideal detector or 10 eV for another, respectively. Descriptions of target atoms are the same as those in Fig. 1. It is shown that a photon detector with resolution better than 10 eV (e.g., a usual bent-crystal spectrometer) is able to distinguish the different theoretical descriptions of target atoms.

asymmetry parameter to the REC line profile, which is illustrated schematically in Fig. 1(a) and also defined as follows by means of the full width at half maximum (FWHM) and its left (LWHM) and right (RWHM) half:

$$A_{1/2} = \frac{\mathrm{RWHM} - \mathrm{LWHM}}{\mathrm{FWHM}}. \tag{6}$$

In Fig. 3, we plot the presently obtained asymmetry parameters $A_{1/2}$ of the REC line profile as a function of projectile energy. In an energy spectrum, the effect of a real x-ray detector can be considered as a mapping from a δ function to a finite-width Gaussian distribution, while the FWHM of the Gaussian distribution is usually defined as detector resolution. The detector resolution, denoted as FWHM$_D$, is assumed to be 0 eV for an ideal detector or 10 eV for another, respectively. As shown in the figure, if the resolution reaches 10 eV or even better, the hydrogenlike and Hartree-Fock descriptions to the wave function of target atoms can be distinguished in the proposed energy region. This can be achieved by a usual bent-crystal spectrometer.

The limited ion-beam monochromaticity is also considered. A practical ion beam is usually prepared by a pair of collimation slits in front of and behind a dipole magnet, and hence only the central part of the beam is allowed to pass through. As a consequence, the energy of projectile ions in the beam exhibits an approximately uniform distribution around the central energy. The present calculation also shows a similar result, as shown in Fig. 1, and suggests that a monochromaticity better than ±5% is enough to distinguish the different descriptions of target wave function. For usual ion accelerators, the typical value of monochromaticity is about ±1%.

The REC photon angular distribution is related to the distribution of the transverse momentum of the target electron in the projectile frame. Thus, the uncertainty of the transverse momentum of the projectile ions itself, in the laboratory frame, may diminish the sensitivity of the angular distribution as a probe of the transition dynamics. In order to make comparison with experiments easily, let

$$D_{10^\circ} = \left(\frac{d\sigma}{d\Omega}\right)_{10^\circ} \Big/ \left(\frac{d\sigma}{d\Omega}\right)_{90^\circ} - \sin^2(10^\circ) \tag{7}$$

denote the deviation of the angle-differential cross sections from the $\sin^2\theta_t$ law at the observation angle 10°. For the different descriptions, the obtained deviations are plotted in Fig. 4 as functions of ion energy. In calculating these deviations, the transverse momentum $p_\perp$ is treated as a uniform distribution in the region ±5% of $p_\perp/p$, where p is the average longitudinal ion momentum. The present results show that an uncertainty ±5% of $p_\perp/p$ is sufficient to distinguish the different theoretical descriptions. In practice, $p_\perp/p$ can be readily controlled within ±2% by beam collimators.

Currently, a low-energy heavy-ion accelerator is under construction, which is devoted to intense HCI beams in the

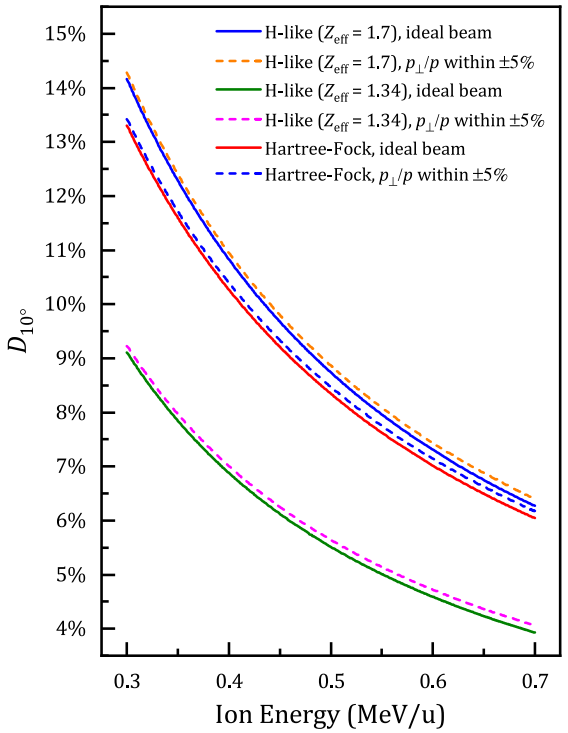

FIG. 4. Influence of ion-beam transverse momentum uncertainty on the angular distribution of the REC photons. The parameter $D_{10°}$ is defined by Eq. (7). It is shown that an uncertainty ±5% of $p_\perp/p$ is acceptable to distinguish the different descriptions of target atoms.

energy region 0.3–0.7 MeV/u [41]. In the near future, it will be equipped with a next-generation 45-GHz superconducting ECRIS. After magnetic analysis and collimations, a bare Ar^{18+} ion beam with monochromaticity better than 0.5% and intensity up to several microampere is expected [41]. Meanwhile, a cryogenic helium jet target with a thickness of 10^{14-16} atoms/cm^2 is already available [53,54]. For line profile measurement, the acceptance of a typical bent-crystal x-ray spectrometer with a resolution of a few eV and energy range covering 4–5 keV is about 10^{-6} of the 4π solid angle [42–44]. Commercial silicon-drifted x-ray detectors for angular distribution measurement usually have a sensitive area of 25-50 mm^2 and consequently give rise to an acceptance of about 10^{-5} of the 4π solid angle [45]. A precise line profile measurement needs to accumulate 10^5-10^6 photons (e.g., 200–500 channels with a channel width of 2–5 eV, each of which accumulates an average of about 10^3 photons), which requires a beam time of about 500 h. And, to obtain a good angular distribution, the estimated beam time is about 100 h.

IV. CONCLUSION

In conclusion, it has been shown that the asymmetry of the K-REC line profile and the deviation of the angular distribution from the $\sin^2\theta_t$ law are magnified in sub-MeV/u collisions. Therefore, we propose to measure the line profile and the angular distribution in collisions of 0.3–0.7-MeV/u Ar^{18+} with helium by using a new-generation intense-beam low-energy heavy-ion accelerator. We note that the present theoretical estimation is not an accurate prediction for experiments but just a proof for the advantage of low-energy REC experiments. New treatment of the REC process in the low-energy region (e.g., the RIA [51,52] approach) is eagerly expected. Accurate measurement of the REC line profile and angular distribution at low energies can serve as a sensitive probe to test future REC theories, especially when the impulse approximation does not hold well.

Key requirements for the proposed experiment, such as the energy resolution of the photon detectors and the energy monochromaticity of ion beams, have been estimated. With the use of a usual bent-crystal spectrometer and a group of commercial silicon-drift x-ray detectors, one will be able to obtain a sufficiently precise line profile and angular distribution, which can be employed to distinguish different REC theories beyond the impulse approximation that has so far been employed. Moreover, accurate REC experiments in the sub-MeV/u energy region may provide insights into interatomic electromagnetic transitions.

ACKNOWLEDGMENTS

We thank Z. Wu, B. Yang, K. N. Lyashchenko, and J. Evslin for carefully reading the manuscript. This work was supported by the National Key Research and Development Program of China under Grant No. 2017YFA0402300 and the National Natural Science Foundation of China under Grant No. 11774356.

[1] J. Eichler, Phys. Rep. **193**, 165 (1990).
[2] J. Eicher and W. E. Meyerhof, *Relativistic Atomic Collisions* (Academic, New York, 1995).
[3] J. Eichler and Th. Stöhlker, Phys. Rep. **439**, 1 (2007).
[4] G. Raisbeck and F. Yiou, Phys. Rev. A **4**, 1858 (1971).
[5] H. W. Schnopper, H. D. Betz, J. P. Delvaille, K. Kalata, A. R. Sohval, K. W. Jones, and H. E. Wegner, Phys. Rev. Lett. **29**, 898 (1972).
[6] P. Kienle, M. Kleber, B. Povh, R. M. Diamond, F. S. Stephens, E. Grosse, M. R. Maier, and D. Proetel, Phys. Rev. Lett. **31**, 1099 (1973).
[7] R. Anholt, S. A. Andriamonje, E. Morenzoni, C. Stoller, J. D. Molitoris, W. E. Meyerhof, H. Bowman, J. S. Xu, Z. Z. Xu, J. O. Rasmussen, and D. H. H. Hoffmann, Phys. Rev. Lett. **53**, 234 (1984).
[8] S. Andriamonje, M. Chevallier, C. Cohen, J. Dural, M. J. Gaillard, R. Genre, M. Hage-Ali, R. Kirsch, A. L'Hoir, B. Mazuy, J. Mory, J. Moulin, J. C. Poizat, J. Remillieux, D. Schmaus, and M. Toulemonde, Phys. Rev. Lett. **59**, 2271 (1987).
[9] Th. Stöhlker, H. Geissel, H. Irnich, T. Kandler, C. Kozhuharov, P. H. Mokler, G. Münzenberg, F. Nickel, C. Scheidenberger, T. Suzuki, M. Kucharski, A. Warczak, P. Rymuza, Z. Stachura, A. Kriessbach, D. Dauvergne, B. Dunford, J. Eichler, A. Ichihara, and T. Shirai, Phys. Rev. Lett. **73**, 3520 (1994).

[10] Th. Stöhlker, C. Kozhuharov, P. H. Mokler, A. Warczak, F. Bosch, H. Geissel, R. Moshammer, C. Scheidenberger, J. Eichler, A. Ichihara, T. Shirai, Z. Stachura, and P. Rymuza, Phys. Rev. A **51**, 2098 (1995).
[11] Th. Stöhlker, F. Bosch, A. Gallus, C. Kozhuharov, G. Menzel, P. H. Mokler, H. T. Prinz, J. Eichler, A. Ichihara, T. Shirai, R. W. Dunford, T. Ludziejewski, P. Rymuza, Z. Stachura, P. Swiat, and A. Warczak, Phys. Rev. Lett. **79**, 3270 (1997).
[12] Th. Stöhlker, T. Ludziejewski, F. Bosch, R. W. Dunford, C. Kozhuharov, P. H. Mokler, H. F. Beyer, O. Brinzanescu, B. Franzke, J. Eichler, A. Griegal, S. Hagmann, A. Ichihara, A. Krämer, J. Lekki, D. Liesen, F. Nolden, H. Reich, P. Rymuza, Z. Stachura, M. Steck, P. Swiat, and A. Warczak, Phys. Rev. Lett. **82**, 3232 (1999).
[13] Th. Stöhlker, X. Ma, T. Ludziejewski, H. F. Beyer, F. Bosch, O. Brinzanescu, R. W. Dunford, J. Eichler, S. Hagmann, A. Ichihara, C. Kozhuharov, A. Krämer, D. Liesen, P. H. Mokler, Z. Stachura, P. Swiat, and A. Warczak, Phys. Rev. Lett. **86**, 983 (2001).
[14] S. Tashenov, Th. Stöhlker, D. Banaś, K. Beckert, P. Beller, H. F. Beyer, F. Bosch, S. Fritzsche, A. Gumberidze, S. Hagmann, C. Kozhuharov, T. Krings, D. Liesen, F. Nolden, D. Protic, D. Sierpowski, U. Spillmann, M. Steck, and A. Surzhykov, Phys. Rev. Lett. **97**, 223202 (2006).
[15] M. Nofal, S. Hagmann, Th. Stöhlker, D. H. Jakubassa-Amundsen, C. Kozhuharov, X. Wang, A. Gumberidze, U. Spillmann, R. Reuschl, S. Hess, S. Trotsenko, D. Banas, F. Bosch, D. Liesen, R. Moshammer, J. Ullrich, R. Dörner, M. Steck, F. Nolden, P. Beller, H. Rothard, K. Beckert, and B. Franczak, Phys. Rev. Lett. **99**, 163201 (2007).
[16] C. R. Vane, H. F. Krause, S. Datz, P. Grafström, H. Knudsen, C. Scheidenberger, and R. H. Schuch, Phys. Rev. A **62**, 010701(R) (2000).
[17] D. Yu, Y. Xue, C. Shao, Z. Song, R. Lu, F. Ruan, W. Wang, J. Chen, B. Yang, Z. Yang, J. Wan, C. Dong, and X. Cai, Nucl. Instrum. Methods Phys. Res. B **269**, 692 (2011).
[18] J. S. Briggs and K. Dettmann, Phys. Rev. Lett. **33**, 1123 (1974).
[19] M. Kleber and D. H. Jakubassa, Nucl. Phys. A. **252**, 152 (1975).
[20] A. R. Sohval, J. P. Delvaille, K. Kalata, and H. W. Schnopper, J. Phys. B **9**, L47 (1976).
[21] R. Shakeshaft and L. Spruch, Phys. Rev. Lett. **38**, 175 (1977).
[22] E. Spindler, H. D. Betz, and F. Bell, J. Phys. B **10**, L561 (1977).
[23] H. Tawara, P. Richard, and K. Kawatsura, Phys. Rev. A **26**, 154 (1982).
[24] M. Gorriz, J. S. Briggs, and S. Alston, J. Phys. B **16**, L665 (1983).
[25] R. Anholt and J. Eichler, Phys. Rev. A **31**, 3505 (1985).
[26] A. Ichihara, T. Shirai, and J. Eichler, Phys. Rev. A **49**, 1875 (1994).
[27] J. Eichler, A. Ichihara, and T. Shirai, Phys. Rev. A **51**, 3027 (1995).
[28] A. Ichihara, T. Shirai, and J. Eichler, Phys. Rev. A **54**, 4954 (1996).
[29] J. Eichler, A. Ichihara, and T. Shirai, Phys. Rev. A **58**, 2128 (1998).
[30] A. B. Voitkiv and N. Grün, J. Phys. B **34**, 321 (2001).
[31] J. Eichler and A. Ichihara, Phys. Rev. A **65**, 052716 (2002).
[32] A. B. Voitkiv and N. Grun, J. Phys. B **35**, 2593 (2002).
[33] A. Surzhykov, S. Fritzsche, Th. Stöhlker, and S. Tashenov, Phys. Rev. Lett. **94**, 203202 (2005).
[34] A. Surzhykov, S. Fritzsche, Th. Stöhlker, and S. Tashenov, Radiat. Phys. Chem. **75**, 1767 (2006).
[35] A. Surzhykov, U. D. Jentschura, Th. Stöhlker, and S. Fritzsche, Phys. Rev. A **73**, 032716 (2006).
[36] A. B. Voitkiv, Phys. Rev. A **73**, 052714 (2006).
[37] S. Fritzsche, A. Surzhykov, and G. Gaigalas, Radiat. Phys. Chem. **76**, 612 (2007).
[38] A. N. Artemyev, A. Surzhykov, S. Fritzsche, B. Najjari, and A. B. Voitkiv, Phys. Rev. A **82**, 022716 (2010).
[39] Th. Stöhlker, P. H. Mokler, K. Beckert, F. Bosch, H. Eickhoff, B. Franzke, M. Jung, T. Kandler, O. Klepper, C. Kozhuharov, R. Moshammer, F. Nolden, H. Reich, P. Rymuza, P. Spädtke, and M. Steck, Phys. Rev. Lett. **71**, 2184 (1993).
[40] Th. Stöhlker, T. Ludziejewski, H. Reich, F. Bosch, R. W. Dunford, J. Eichler, B. Franzke, C. Kozhuharov, G. Menzel, P. H. Mokler, F. Nolden, P. Rymuza, Z. Stachura, M. Steck, P. Swiat, A. Warczak, and T. Winkler, Phys. Rev. A **58**, 2043 (1998).
[41] L. Sun, H. W. Zhao, W. Lu, J. W. Guo, Y. Yang, H. Jia, L. Lu, and W. Wu, X-Ray Spectrosc. **49**, 47 (2020).
[42] J. Hoszowska, J. C. Dousse, J. Kern, and C. Rhême, Nucl. Instrum. Methods Phys. Res. A **376**, 129 (1996).
[43] I. Ismail, L. Journel, R. Vacheresse, O. Travnikova, T. Marin, D. Céolin, R. Guillemin, T. Marchenko, M. Zmerli, D. Koulentianos, R. Püttner, J. Palaudoux, F. Penent, and M. Simon, Rev. Sci. Instrum. **92**, 073104 (2021).
[44] Z. Yang, Z. Zhang, M. Lv, Z. Hu, Z. An, M. Wei, Y. Zhao, and J. Yang, Measur. Sci. Technol. **32**, 047001 (2021).
[45] Silicon Drift Detector, https://www.amptek.com/products/x-ray-detectors/fastsdd-x-ray-detectors-for-xrf-eds/fastsdd-silicon-drift-detector.
[46] D. P. Dewangan and J. Eichler, Phys. Rep. **247**, 59 (1994).
[47] P. P. Kane, Phys. Rep. **218**, 67 (1992).
[48] A. B. Voitkiv, B. Najjari, N. Toshima, and J. Ullrich, J. Phys. B **39**, 3403 (2006).
[49] A. Simon, A. Warczak, T. ElKafrawy, and J. A. Tanis, Phys. Rev. Lett. **104**, 123001 (2010).
[50] D. S. La Mantia, P. N. S. Kumara, S. L. Buglione, C. P. McCoy, C. J. Taylor, J. S. White, A. Kayani, and J. A. Tanis, Phys. Rev. Lett. **124**, 133401 (2020).
[51] D. Belkić, Nucl. Instrum. Methods Phys. Res. B **99**, 218 (1995).
[52] D. Belkic, Phys. Scr. **53**, 414 (1996).
[53] H. W. Becker, L. Buchmann, J. Görres, K. U. Kettner, H. Kräwinkel, C. Rolfs, P. Schmalbrock, H. P. Trautvetter, and A. Vlieks, Nucl. Instrum. Methods **198**, 277 (1982).
[54] K. Schmidt, K. A. Chipps, S. Ahn, D. W. Bardayan, J. Browne, U. Greife, Z. Meisel, F. Montes, P. D. O'Malley, W. J. Ong, S. D. Pain, H. Schatz, K. Smith, M. S. Smith, and P. J. Thompson, Nucl. Instrum. Methods Phys. Res. A **911**, 1 (2018).